THE JOURNAL OF PHYSICAL CHEMISTRY C

Article

pubs.acs.org/JPCC

Controlling Wettability of Boron Nitride Nanotube Films and Improved Cell Proliferation

Ling Li,[†,‡] Lu Hua Li,*[,†] Sugeetha Ramakrishnan,[§] Xiujuan J. Dai,[†] Kevin Nicholas,[§] Ying Chen,*[,†] Zhiqiang Chen,[†] and Xiaowei Liu[‡]

[†]Institute for Frontier Materials, Deakin University, Geelong Waurn Ponds Campus, Waurn Ponds, Victoria 3216, Australia

[‡]MEMS Center, Harbin Institute of Technology, Harbin 150001, P. R. China

[§]BioDeakin, Deakin University, Geelong Waurn Ponds Campus, Waurn Ponds, Victoria 3216, Australia

S *Supporting Information*

ABSTRACT: Desired wettability has been achieved on highly hydrophobic boron nitride nanotube (BNNT) films using nitrogen/hydrogen (N_2/H_2) gas plasma treatments under controlled input energies and modes. Both hydrophilicity (contact angle (CA) ~60°) and superhydrophilicity (CA < 5°) are demonstrated on BNNT films with little change of the surface morphology or the structure of individual BNNTs. The combination of continuous wave and pulse mode (CW+P) plasma shows more effective wettability modification and introduces more amine functional groups than the continuous wave (CW) plasma alone at a given input energy. (Super)-hydrophilic/hydrophobic patterns have been created on BNNT films using masked plasma methods. The cell response to BNNT films is investigated for the first time. The proliferation of human primary mammary fibroblasts and a transformed mammary cell line (TXP RFP3) shows that the untreated hydrophobic BNNT films can support the growth of both cell lines, but the plasma treatments greatly enhance (up to six times) the number of cells attached to the surface of BNNT films.

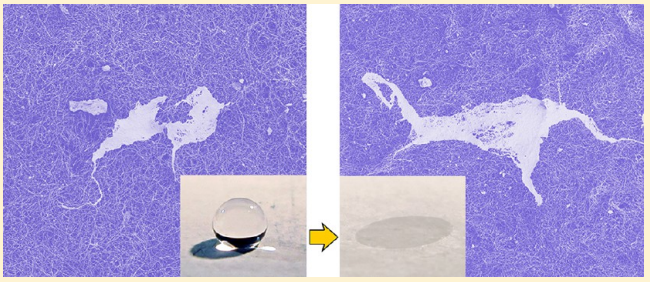

INTRODUCTION

Boron nitride nanotubes (BNNTs) have many similarities to carbon nanotubes (CNTs), such as similar structures, superior mechanical properties, and excellent thermal conducting capability,[1,2] but they also possess many properties unavailable in their carbon counterparts. BNNTs are more stable and electrically insulating.[3−5] BNNTs are promising deep ultraviolet light emitters and potential candidates for building optoelectronic devices.[6] The growth of nanotube films on different substrates further broadens their applications.[7,8] As-grown BNNT films are normally nonwettable to water due to the nanoroughness enabled Cassie state as well as adsorbed hydrocarbon contaminations, and therefore, they are usable in applications requiring strong water-repellence.[9−11] However, many other applications need highly wettable BNNT films. When BNNT films are used to reinforce polymer composites, it is essential to turn (super)hydrophobic BNNT films to hydrophilic. This wettability change can reduce void defects in composites and enhance interfacial bindings between BNNTs and matrix. In another case, BNNTs are highly efficient in desalination due to their excellent ion-selectivity,[12,13] and this application requires hydrophilic BNNTs or their films to allow water to pass through tubes. Many biological applications also require (super)hydrohilic film surfaces, because cells have difficulty to attach to hydrophobic films.[14] In addition, it is found that hydrophobic nanomaterials show higher cytotoxicity than hydrophilic ones.[15]

According to the studies on CNTs, films of CNTs show better cell viability than dispersed CNTs, which are found to inhibit cell proliferation.[16] In contrast to the large number of cell studies on CNT films, the bioapplication of BNNT films has not been investigated yet. Actually, BNNT films, similar to CNT films, have huge roughness, which is beneficial for strong cell attachment, and a nanoporous three-dimensional structure suitable for tissue scaffolding and engineering. Different from the potential toxicity of CNTs that prevents their large-scale use,[17] most studies have found that BNNTs are cytocompatible and safe in different living organisms.[18−21] Other bioapplications of BNNTs or BNNT reinforced composite have also been proposed recently.[22−24] In addition, BNNTs should be more stable in bioenvironment due to their higher chemical and pH resistances than CNTs. Still, wettability modification is important for applying BNNT films in bioapplications.

Although wettability modification of CNT films has been extensively investigated, such study has seldom been conducted on BNNT films. Recently UV−ozone treatments were used to change the wetting properties of BNNT films, which had been

Received: June 22, 2012
Revised: July 30, 2012
Published: August 2, 2012

   dx.doi.org/10.1021/jp306148e | *J. Phys. Chem. C* 2012, 116, 18334−18339

attributed to the removal of hydrocarbon contaminations on the BNNT surfaces.[11,25] There are three methods proposed on the modification of powder-like BNNTs for improving their liquid dispersion: polymer wrapping,[26−29] covalent functionalization in solution,[30,31] and plasma treatment.[32,33] The first two methods usually involve sonication and are not suitable for treating BNNT films.

Here, we demonstrate a room-temperature nitrogen/hydrogen (N_2+15%H_2) mixture gas plasma treatment using continuous wave (CW) and a combination of continuous and pulsed (CW+P) modes to tune highly hydrophobic BNNT films to (super)hydrophilic. The tailored plasma conditions ensured little damage on individual BNNTs as well as the physical/surface structure of BNNT films, while different N-containing functional groups, including amine, amide, and imine (nitrile), could be introduced. The plasma method was also used to create (super)hydrophilic patterns on hydrophobic BNNT film surfaces. The potential bioapplications of BNNT films have been explored for the first time using human mammary fibroblasts and a transformed mammary cell line (TXP RFP3). No obvious cytotoxicity of BNNT films was observed, and the cell proliferation was much more preferable on the plasma treated films.

EXPERIMENTAL METHODS

BNNT Film Growth. Films of high density and purity BNNTs were grown on steel substrates (1−4 cm^2) using the boron (B) ink method.[8,10] In this process, amorphous B powder (95%−97%, Fluka) was first ball-milled in argon (Ar) gas at 300 kPa for 150 h. The milled powder was then dispersed in a ferric nitrate ($Fe(NO_3)_3{\cdot}9H_2O$, 98%, Pronalys) ethanol solution under bath sonication for 0.5 h to form B ink. The B ink was brushed on steel substrates and heated at 1100 °C in N_2+15%H_2 gas for 1 h to form BNNT films.

Plasma Treatments. Low pressure plasma treatment was carried out in a purpose-built reactor. The system has an inductively coupled radio frequency (RF, 13.56 MHz) plasma reactor, a cylindrical glass reaction chamber enclosed in a Faraday cage, and an antenna around the chamber inlet to transfer RF power to the reaction area. Plasma treatments were operated in either CW or continuous plus pulsed (CW+P) mode. The CW mode has a plasma power of 100 W. The P mode plasma has a rectangular function with a peak power of 100 W and a duty cycle of 10% (DC = $T_{on}/T_{on} + T_{off}$, T_{on} = 1 ms). The surfaces of all samples were pretreated using CW Ar gas plasma for 1 min for surface activation and cleaning purposes. During N_2 + 15%H_2 gas plasma treatment, the pressure was maintained constant at 5.5 × 10^{-2} mbar. Hydrophobic and (super)hydrophilic patterns were made by covering a metal film decorated with 2 mm diameter holes on the BNNT films. The reason for choosing N_2 + 15%H_2 gas is that the admixture is more chemically reactive than nitrogen alone and better enhances the selectivity and quantity of amino functional groups to build a stable structure.[34] With the help of hydrogen, amine or amide groups can covalently incorporate to BNNTs through B−N bonds.[32,35]

Characterization Methods. Scanning electron microscopy (SEM) images were taken using LEO 1530 and Supra 55 V instruments. Transmission electron microscopy (TEM) studies used a JEOL-2010F machine. Wettability was investigated using a contact angle and surface tension tester (CAM101, KSV). The Young−Laplace equation was used to curve-fit drop profiles captured by an attached camera. Deionized water droplets with a volume of 3−5 μL were used. Contact angle (CA) results are average values based on five to eight measurements at different locations. Hydrocarbon contaminations on the BNNT films were investigated using a Bruker Vertex 70 FTIR system in reflectance (ATR) mode immediately after the plasma treatments. Surface functionalization was measured using a K-alpha X-ray photoelectron spectroscopy (XPS, Thermo Fischer Scientific) system, with a monochromatic X-ray of a spot size of 400 μm. A flood gun was used to compensate charges due to the insulating nature of BNNTs. Pass energies of 100 and 20 eV were used in survey and high resolution scans, respectively. All XPS data were corrected using the binding energy (BE) position of C−C at 284.6 eV. The quantity of primary amine function groups was determined by the 4-(trifluoromethyl)benzaldehyde (TFBA) derivatization method, in which the BNNT films reacted with excessive TFBA and the percentages of primary amine were calculated based on the contents of fluorine analyzed by XPS:[36]

$$[NH_2] = \left[\frac{[F]}{3}/[B]\right] \times 100\%$$

Cell Culture, Counting, and Imaging. Two different cell lines were used in this study: human primary mammary fibroblasts and a transformed breast tumor cell line (TXP RFP3). TXP RFP3 cells were cultured in Dulbecco's modified eagle medium (DMEM with high glucose) with 10% fetal bovine serum (FBS), 1% L-glutamine, and 1% penicillin/streptomycin. Human mammary fibroblasts were cultured in fibroblast medium (Sciencell, USA) supplemented with 2% fetal bovine serum (FBS), 1% fibroblast growth supplement (FGS), and 1% penicillin/streptomycin. Both cell types were seeded at a density of 1 × 10^5 cells on a 35 mm diameter cell culture plate (made of tissue culture grade polystyrene supporting 100% cell adhesion), untreated BNNT films (hydrophobic), and 5CW+10P and 10CW plasma treated BNNT films (superhydrophilic). The cells were allowed to proliferate in a controlled environment (37 °C, humidified and 5% CO_2) for 48 h (TXP RFP3) and 96 h (fibroblasts), respectively. A similar procedure was followed to determine cell growth and proliferation of both cells. Cells on both the culture plates and the substrates were removed and analyzed for cell number. To count cells on the plate, 0.5 mL of 0.5% trypsin/EDTA was added to each well, cells were incubated for 2 min, and then 1.5 mL of fresh media was added to the wells to deactivate trypsin (a total volume of 2 mL). An aliquot (10 μL) was mixed with tryphan blue (dye), and the number of cells was counted using a hemocytometer. To count the number of cells on BNNT films, each film was transferred to a new culture dish, 1 mL of trypsin was added, and the samples were incubated for 2 min. Fresh media (2 mL) was added to deactivate trypsin (a total volume of 3 mL). The cells present on each film were calculated as cells per cm^2 surface area. The analysis of cell number was repeated 5 times for each film. Values for each treatment were analyzed using a t test and significant differences shown at $P < 0.05$. For SEM imaging, the cells were washed once with PBS, fixed with 4% paraformaldehyde, and dehydrated with increasing grades of ethanol, from 60 to 100%. The samples were then dried overnight, followed by sputter coating with gold.

dx.doi.org/10.1021/jp306148e | J. Phys. Chem. C 2012, 116, 18334−18339

RESULTS AND DISCUSSION

Wettability Control of Boron Nitride Nanotube Films. High purity BNNT films were used for plasma treatments, and the film thickness was in the range of 20−40 μm.[10] The majority of the BNNTs have a bamboo-like structure, along with some cylindrical nanotubes. The average contact angle of the untreated films was 158.1 ± 3.6°. Ar gas CW mode plasma with an energy input of 100 W·min (for 1 min) was used to activate the BNNT surfaces first, which can help to enhance plasma functionalization in further treatments. The short pretreatment reduced the CA by less than 6° (to 152.5 ± 2.8°) but did not change the surface morphology of the films (therefore no roughness change), as shown by both SEM and the aging results (after 100 h of aging in air, the CA returned to 157.9 ± 6.0°) (see Supporting Information, Figure S1 for SEM images). This small CA decrease may be due to the removal of hydrocarbon on the BNNTs as well as the possible formation of a small amount of polar oxygen functional groups originating from the oxygen impurities in the Ar gas source and atmospheric oxygen.[37,38] Wettability modification by N_2 + 15% H_2 gas plasma was tested using different plasma input energies and modes. CW plasma for 5 min (5CW), with a relatively small input energy of 500 W·min, turned the BNNT films to hydrophilic with a CA down to 65.2 ± 4.2°. After CW plasma for 10 min (10CW) with a large energy of 1000 W·min, the BNNT films became superhydrophilic with CAs < 5°. Superhydrophilicity can also be achieved using CW+P mode plasma with an input energy of 600 W·min (CW plasma for 5 min and P plasma for 10 min, 5CW+10P). The CA changes after these treatments are summarized in Figure 1.

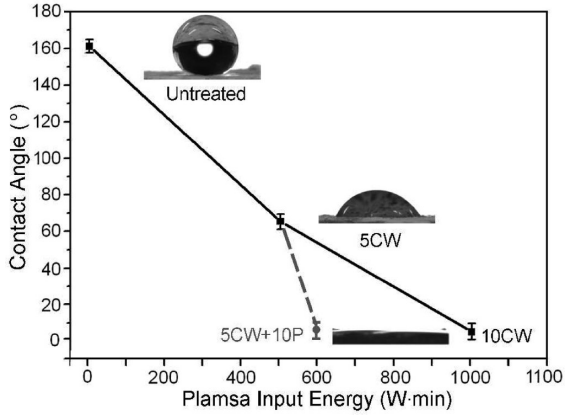

Figure 1. Contact angle changes of BNNT films from highly hydrophobic to hydrophilic and superhydrophilic after N_2/H_2 plasma treatments with different energy inputs and modes.

(Super)hydrophilic patterns on highly hydrophobic BNNT films were successfully produced using the N_2/H_2 gas plasma. Figure 2a shows that while most of a BNNT film remained nonwettable, indicated by a round water droplet sitting on the surface (left), one small portion of the film became superwettable to water (right and arrowed). This superhydrophilic pattern was produced by treating the BNNT film covered with a metal mask decorated with holes using 5CW+10P plasma. Less hydrophilic patterns with CAs ~ 60° on BNNT films were realized using 5CW plasma (Figure 2b). BNNT films with these patterns may be usable in droplet manipulation, lab-on-a-chip, and biological tests.[39]

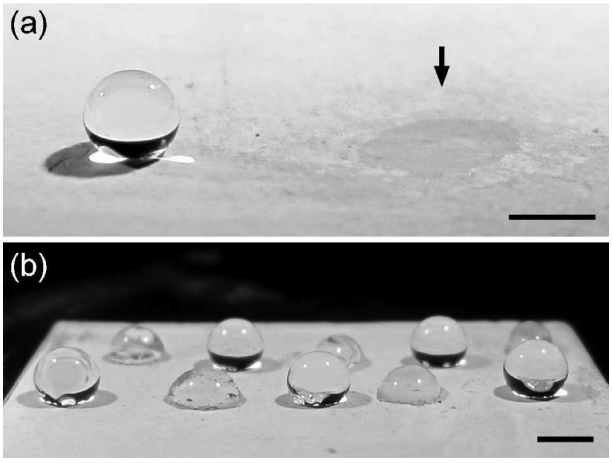

Figure 2. Photos of (super)hydrophilic patterns on hydrophobic BNNT films created by masked plasma treatments: (a) 5CW+10P (a superhydrophilic spot arrowed) and (b) 5CW. Scale bars 2 mm.

Normally wettability changes are associated with physical and/or chemical changes, and these two aspects are inspected respectively. The possible physical changes (i.e., roughness) of the film surfaces caused by the plasma were investigated on the 10CW treated films which had the maximum energy input (1000 W·min) among the three plasma conditions. SEM was used to qualitatively show the possible change of film surfaces induced by the plasma. Figure 3 compares the SEM images of

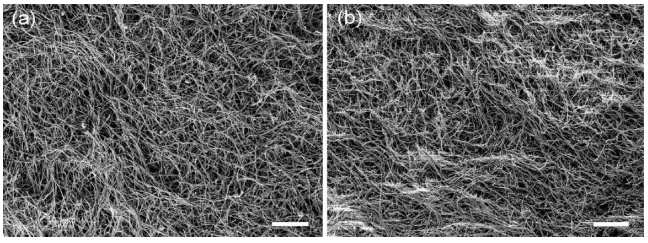

Figure 3. SEM images of the same location of a BNNT film (a) before and (b) after 10CW N_2+15%H_2 plasma treatment. Scale bars 10 μm.

the same area of a BNNT film before and after 10CW treatment. The film surface basically kept its original appearance and roughness, though some nanotubes slightly bundled after the treatment. The surface structure of individual nanotubes after 10CW treatment was investigated using TEM (Figure 4). Most of the nanotube structures were well retained, though slight damages were sometimes found on a few outer layers of the BNNTs. The almost intactness of individual BNNTs is due to the used 100 W RF power, whose electron energy distribution function only shows a modest high energy tail. This specifically chosen power is low enough to minimize the damage on BNNTs while it still allows surface modification/functionalization to happen.[33] Therefore, the used plasma even at its highest energy input does not change the physical structure of the films.

It was recently found that hydrocarbon contaminations on BNNTs could partly contribute to hydrophobicity of BNNTs and their films.[11,25] So the contents of hydrocarbon on the BNNT films were examined before and after different plasma treatments using ATR-FTIR spectroscopy. The FTIR results in Figure 5 reveal that the hydrocarbon contaminations were dramatically reduced after the plasma treatments, as reflected

dx.doi.org/10.1021/jp306148e | J. Phys. Chem. C 2012, 116, 18334−18339

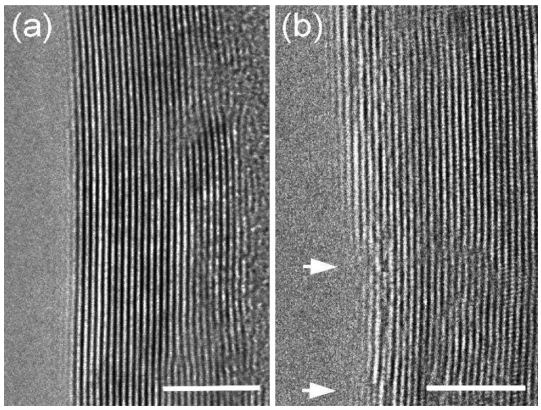

Figure 4. HRTEM images of BNNTs (a) before and (b) after 10CW N_2+15%H_2 plasma treatment. The damage induced by the plasma was arrowed. Scale bars 5 nm.

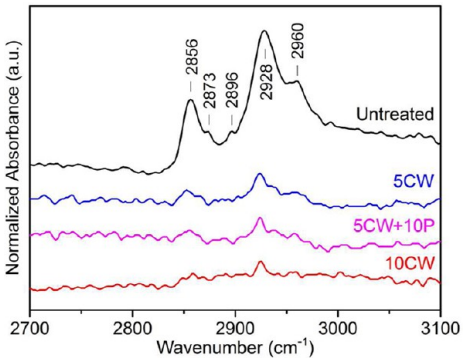

Figure 5. ATR-FTIR spectra showing the dramatically reduced levels of hydrocarbon surface contaminations on untreated and 5CW, 5CW +10P, and 10CW N_2+15%H_2 plasma treated BNNT films.

by the almost disappearances of the 2928 and 2856 cm^{-1} bands representing asymmetric and symmetric C−H vibrations, respectively.[11] Therefore, the increased wettability of the BNNT films after the plasma treatments can be partly attributed to the removal of the hydrocarbon contaminations. This, however, cannot explain the different CA values after different plasma treatments (e.g., the 5CW+10P treated films are much more hydrophilic than the 5CW treated ones), because the hydrocarbon levels after the 5CW, 5CW+10P, and 10CW treatments are very similar (Figure 5). XPS was then utilized to investigate the surface functionalization induced by the plasma. Before the plasma treatment, the B 1s and N 1s core-level photoemission spectra of the films show a typical B−N peak at BEs of 190.1 and 398.1 eV, respectively (upper row, Figure 6). After 5CW+10P plasma treatments (middle row, Figure 6), a shoulder at 191.3 eV appears in the B 1s spectrum, which corresponds to B bonded in a ternary BN_xO_y species (purple).[40] The additional peaks at 399.0 and 400.2 eV in the N 1s spectrum indicate the formation of amine (red) and amide (blue) bonds.[41,42] The 10CW plasma (lower row, Figure 6) also creates BN_xO_y species as shown in the B 1s spectrum, but gives a slightly different N 1s profile that indicates the formation of more amide than amine groups. The C 1s spectra of the two plasma treated films verify the existence of amide (288.1 eV) and amine (285.8 eV), but also indicate the presence of imine (nitrile) (286.7 eV).[33,43] Consistent with the N 1s spectra, the C 1s spectra show that the CW+P mode grafts more amine groups on the BNNTs, while the CW mode, on

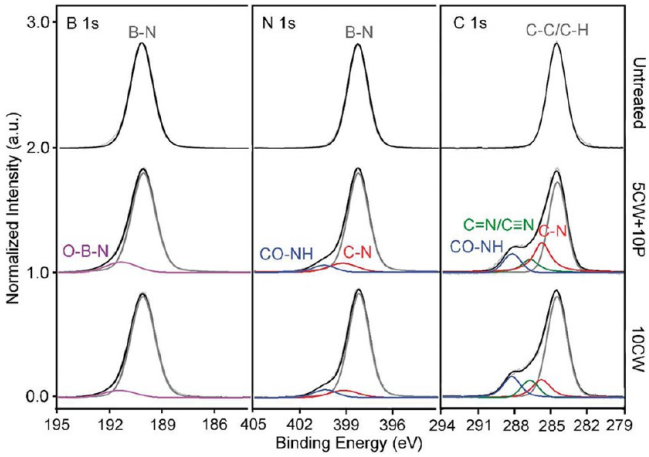

Figure 6. B 1s, N 1s, and C 1s regions of the XPS spectra of BNNT films before plasma treatment (upper row) and after 5CW+10P plasma treatment (middle row) and 10CW treatment (lower row). In the fittings: purple, BN_xO_y; blue, amide; red, amine; green, imine (nitrile).

the other hand, forms more amide. The primary amines ($-NH_2$) content of the 5CW+10P treated films was 2.09%, determined by TFBA.[36] This difference can be understood by the fact that the CW mode plasma with continuous and higher energy inputs supports the dissociation and further reaction of freshly formed amine to form amide and imine with the presence of O and C impurities; while the P mode with much less energy input and off-time can retain more amine.[44,45] Though the energy input of 10CW (1000 W·min) is much higher than that of 5CW+10P (600 W·min), the total amount of functional groups introduced by 10CW is similar to that by 5CW+10P (Figure 6). This explains that the lower energy input 5CW+10P can have a similar effect on modifying the wettability of BNNT films to the 10CW treatment of the high energy input. However, it should be noted that the functional groups introduced by the CW+P mode are more stable on the BNNTs than those by the CW mode, as evidenced by the aging results. The CA of the 5CW+10P treated BNNT films increased to 42.8° after 100 h of aging in air, while the CA of the 10CW treated films jumped back to 81.5°.

Cell Growth on Boron Nitride Nanotube Films. As one example of possible applications of the plasma treated BNNT films, cell proliferation was tested using two representative cell lines: human primary mammary fibroblasts and a transformed cell line TXP RFP3. The cell numbers on unit area of the untreated and different plasma treated BNNT films are compared in Figure 7. The results show that the untreated BNNT films support the growth of both types of cells, but plasma treatments can greatly enhance the number of cells. The increases in cell numbers are most likely due to the change of the BNNT films from hydrophobic to superhydrophilic after plasma treatments, because cells have difficulty to attach to nonwettable surfaces.[14] It has also been reported before that hydrophobic nanomaterials have higher toxicity than hydrophilic ones.[15] The surface functionalization of BNNTs also helped to enhance the cell growth, since functional groups, such as amine and amide, have the ability to covalently couple cells.[46] It is noted that the 10CW plasma treatment results in slightly higher cell numbers than the 5CW+10P treatment, though the 5CW+10P treated films had more primary amine groups which are positively charged and more effective in

dx.doi.org/10.1021/jp306148e | J. Phys. Chem. C 2012, 116, 18334−18339

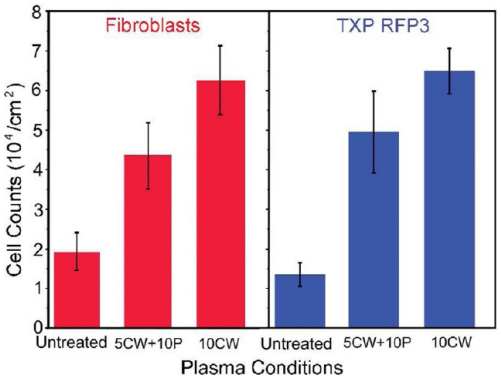

Figure 7. Cell numbers of fibroblasts and TXP RFP3 attached to untreated and 5CW+10P and 10CW N_2+15%H_2 plasma treated BNNT films. Values represent the standard error of the mean and n = 5. Cell numbers on untreated and treated surfaces were significantly different (P < 0.05) for both cell types.

covalent coupling of proteins and biological molecules.[47] This is possibly due to more physical damage on nanotube surfaces by the 10CW treatment.

The morphologies of cells on BNNT films were investigated by SEM. The 5CW+10P and 10CW plasma treated BNNT films result in more prolonged extension of membrane projections (for both cell lines) compared to the untreated films, while no obvious cell shape difference is found between the films treated by 5CW+10P and 10CW plasma (Figure 8). This indicates that the surface of plasma treated BNNT films provides a better support for cell proliferation and viability. Most cells are attached to the prostrate BNNTs and proliferate along the BNNTs, while some BNNTs appear on the surface of the cells. Some cells show a capacity to bundle the BNNTs beneath together to form a "yarn" (Figure 8c), which could be caused by the dehydration process in the SEM sample preparation. This suggests a strong adhesion between the cells and the plasma treated BNNTs. Some cell projections are directed inside the BNNT films to form a three-dimensional structure (arrowed in Figure 8c and f). Based on this study, BNNTs show no obvious toxicity to the tested cells even with a large area of physical contact. This opens new opportunities for exploiting the noncarbon nanostructured surfaces in tissue engineering.

CONCLUSION

Highly hydrophobic BNNT films (158.1°) can be tuned to desired wettability, e.g. hydrophilic (CA ∼ 60°), and superhydrophilic (CA < 5°), using N_2/H_2 gas plasma of different energy inputs and modes. (Super)hydrophilic patterns on hydrophobic BNNT films are demonstrated using masked plasma treatments. The plasma treatment can retain the surface morphology of the nanotube films as well as the layered structure of individual BNNTs. The combination of continuous wave and pulse mode (CW+P) plasma is more effective in changing the wettability and introduced more amine functional groups than the continuous wave (CW) plasma alone. The cell growth tests using human mammary fibroblasts and transformed cell line (TXP RFP3) show that the untreated BNNT films can support the cell growth, but plasma treatments have a great enhancement of cell proliferation. The cell attachment to the BNNT films is strong due to both improved wettability and grafted functional groups introduced by plasma. These results direct further and more detailed investigations of plasma treated BNNT films in tissue scaffolding and engineering.

ASSOCIATED CONTENT

Supporting Information

SEM images of BNNT films before and after the Ar plasma pretreatment. This material is available free of charge via the Internet at http://pubs.acs.org.

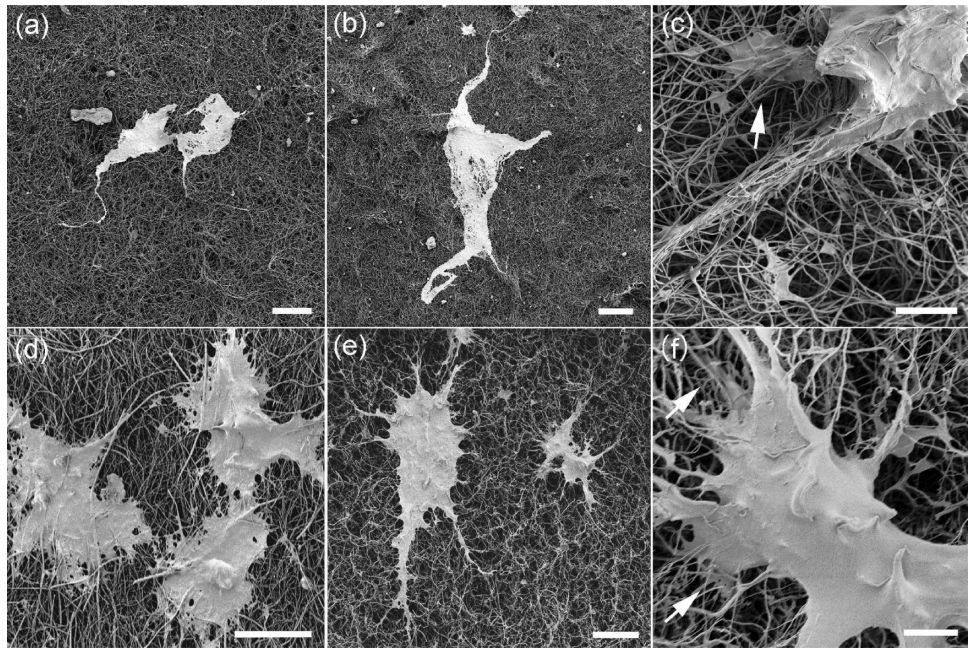

Figure 8. SEM images of fibroblasts on (a) untreated and (b and c) plasma treated BNNT films; and TXP RFP3 cells on (d) untreated and (e and f) plasma treated BNNT films. Scale bars: (a and b) 50 μm; (c) 5 μm; (d and e) 20 μm; (f) 5 μm.

dx.doi.org/10.1021/jp306148e | J. Phys. Chem. C 2012, 116, 18334−18339

AUTHOR INFORMATION

Corresponding Author

*L.H.L.: e-mail, luhua.li@deakin.edu.au; tel, +61-3-52272589; fax, +61-3-52271103. Y.C.: e-mail,ian.chen@deakin.edu.au; tel, +61-3-52273243; fax, +61-3-52271103.

Notes

The authors declare no competing financial interest.

ACKNOWLEDGMENTS

The authors thank Dr. Peter Lamb for manuscript preparation and discussion, as well as scientific and technical assistance from the XPS facility at RMIT University. Financial support from the Australian Research Council under the Centre of Excellence and Discovery programs is gratefully acknowledged.

REFERENCES

(1) Chopra, N. G.; Luyken, R. J.; Cherrey, K.; Crespi, V. H.; Cohen, M. L.; Louie, S. G.; Zettl, A. *Science* **1995**, *269*, 966−967.

(2) Xiao, Y.; Yan, X. H.; Cao, J. X.; Ding, J. W.; Mao, Y. L.; Xiang, J. *Phys. Rev. B* **2004**, *69*, 205415.

(3) Golberg, D.; Bando, Y.; Kurashima, K.; Sato, T. *Scr. Mater.* **2001**, *44*, 1561−1565.

(4) Chen, Y.; Zou, J.; Campbell, S. J.; Le Caer, G. *Appl. Phys. Lett.* **2004**, *84*, 2430−2432.

(5) Zhang, H.; Yu, J.; Chen, Y.; Fitz Gerald, J. *J. Am. Ceram. Soc.* **2006**, *89*, 675−679.

(6) Li, L. H.; Chen, Y.; Lin, M. Y.; Glushenkov, A. M.; Cheng, B. M.; Yu, J. *Appl. Phys. Lett.* **2010**, *97*, 141104.

(7) Ajayan, P. M.; Zhou, O. Z. Applications of carbon nanotubes. In *Carbon Nanotubes*; Dresselhaus, M. S., Dresselhaus, G., Avouris, P., Eds.; Springer: Berlin, 2001; Vol. *80*; pp 391−425.

(8) Li, L. H.; Chen, Y.; Glushenkov, A. M. *J. Mater. Chem.* **2010**, *20*, 9679−9683.

(9) Lee, C. H.; Drelich, J.; Yap, Y. K. *Langmuir* **2009**, *25*, 4853−4860.

(10) Li, L. H.; Chen, Y. *Langmuir* **2010**, *26*, 5135−5140.

(11) Boinovich, L. B.; Emelyanenko, A. M.; Pashinin, A. S.; Lee, C. H.; Drelich, J.; Yap, Y. K. *Langmuir* **2012**, *28*, 1206−1216.

(12) Hilder, T. A.; Gordon, D.; Chung, S. H. *Small* **2009**, *5*, 2183−2190.

(13) Won, C. Y.; Aluru, N. R. *Chem. Phys. Lett.* **2009**, *478*, 185−190.

(14) Curtis, A. S. G.; Forrester, J. V.; Mcinnes, C.; Lawrie, F. *Eur. J. Cell Biol.* **1983**, *97*, 1500−1506.

(15) Tian, F. R.; Cui, D. X.; Schwarz, H.; Estrada, G. G.; Kobayashi, H. *Toxicol. In Vitro* **2006**, *20*, 1202−1212.

(16) Edwards, S. L.; Church, J. S.; Werkmeister, J. A.; Ramshaw, J. A. M. *Biomaterials* **2009**, *30*, 1725−1731.

(17) Lam, C. W.; James, J. T.; McCluskey, R.; Arepalli, S.; Hunter, R. L. *Crit. Rev. Toxicol.* **2006**, *36*, 189−217.

(18) Ciofani, G.; Raffa, V.; Menciassi, A.; Cuschieri, A. *Biotechnol. Bioeng.* **2008**, *101*, 850−858.

(19) Chen, X.; Wu, P.; Rousseas, M.; Okawa, D.; Gartner, Z.; Zettl, A.; Bertozzi, C. R. *J. Am. Chem. Soc.* **2009**, *131*, 890−891.

(20) Ciofani, G.; Danti, S.; D'Alessandro, D.; Moscato, S.; Menciassi, A. *Biochem. Biophys. Res. Commun.* **2010**, *394*, 405−411.

(21) Horváth, L.; Magrez, A.; Golberg, D.; Zhi, C.; Bando, Y.; Smajda, R.; Horváth, E.; Forró, L. s.; Schwaller, B. *ACS Nano* **2011**, *5*, 3800−3810.

(22) Raffa, V.; Ciofani, G.; Cuschieri, A. *Nanotechnology* **2009**, 20.

(23) Lahiri, D.; Rouzaud, F.; Richard, T.; Keshri, A. K.; Bakshi, S. R.; Kos, L.; Agarwal, A. *Acta Biomater.* **2010**, *6*, 3524−3533.

(24) Ciofani, G.; Danti, S.; Genchi, G. G.; D'Alessandro, D.; Pellequer, J. L.; Odorico, M.; Mattoli, V.; Giorgi, M. *Int. J. Nanomed.* **2012**, *7*, 19−24.

(25) Aliev, A.; Boinovich, L.; Bukhovets, V.; Emelyanenko, A.; Gorbunov, A.; Gorodetskii, A.; Pashinin, A. *Nanotechnol. Russ.* **2011**, *6*, 723−732.

(26) Zhi, C. Y.; Bando, Y.; Tang, C. C.; Kuwahara, H.; Golberg, D. *J. Phys. Chem. C* **2007**, *111*, 1230−1233.

(27) Yap, Y. K.; Velayudham, S.; Lee, C. H.; Xie, M.; Blair, D.; Bauman, N.; Green, S. A.; Liu, H. Y. *ACS Appl. Mater. Interfaces* **2010**, *2*, 104−110.

(28) Zhi, C.; Bando, Y.; Tang, C.; Xie, R.; Sekiguchi, T.; Golberg, D. *J. Am. Chem. Soc.* **2005**, *127*, 15996−15997.

(29) Xie, S.-Y.; Wang, W.; Fernando, K. A. S.; Wang, X.; Lin, Y.; Sun, Y.-P. *Chem. Commun.* **2005**, 3670−3672.

(30) Zhi, C.; Bando, Y.; Tang, C.; Honda, S.; Sato, K.; Kuwahara, H.; Golberg, D. *Angew. Chem., Int. Ed.* **2005**, *44*, 7932−7935.

(31) Zettl, A.; Sainsbury, T.; Ikuno, T.; Okawa, D.; Pacile, D.; Frechet, J. M. J. *J. Phys. Chem. C* **2007**, *111*, 12992−12999.

(32) Ikuno, T.; Sainsbury, T.; Okawa, D.; Frehet, J. M. J.; Zettl, A. *Solid State Commun.* **2007**, *142*, 643−646.

(33) Dai, X. J. J.; Chen, Y.; Chen, Z. Q.; Lamb, P. R.; Li, L. H.; du Plessis, J.; McCulloch, D. G.; Wang, X. G. *Nanotechnology* **2011**, *22*, 245301.

(34) Meyer-Plath, A. A.; Finke, B.; Schröder, K.; Ohl, A. *Surf. Coat. Technol.* **2003**, *174*−*175*, 877−881.

(35) Cao, F. L.; Ren, W.; Ji, Y. M.; Zhao, C. Y. *Nanotechnology* **2009**, *20*, 145703.

(36) Choukourov, A.; Kousal, J.; Slavínská, D.; Biederman, H.; Fuoco, E. R.; Tepavcevic, S.; Saucedo, J.; Hanley, L. *Vacuum* **2004**, *75*, 195−205.

(37) Inagaki, N.; Tasaka, S.; Narushima, K.; Kobayashi, H. *J. Appl. Polym. Sci.* **2002**, *85*, 2845−2852.

(38) Dai, X. J. J.; du Plessis, J.; Kyratzis, I. L.; Maurdev, G.; Huson, M. G.; Coombs, C. *Plasma Processes Polym.* **2009**, *6*, 490−497.

(39) Kinoshita, H.; Ogasahara, A.; Fukuda, Y.; Ohmae, N. *Carbon* **2010**, *48*, 4403−4408.

(40) Vincent, H.; Chassagneux, F.; Vincent, C.; Bonnetot, B.; Berthet, M. P.; Vuillermoz, A.; Bouix, J. *Mater. Sci. Eng., A* **2003**, *340*, 181−192.

(41) Khare, B. N.; Wilhite, P.; Quinn, R. C.; Chen, B.; Schingler, R. H.; Tran, B.; Imanaka, H.; So, C. R.; Bauschlicher, C. W.; Meyyappan, M. *J. Phys. Chem. B* **2004**, *108*, 8166−8172.

(42) Felten, A.; Bittencourt, C.; Pireaux, J. J.; Van Lier, G.; Charlier, J. C. *J. Appl. Phys.* **2005**, *98*, 074308.

(43) Poncin-Epaillard, F.; Chevet, B.; Brosse, J.-C. *J. Appl. Polym. Sci.* **1994**, *53*, 1291−1306.

(44) Gengenbach, T. R.; Chatelier, R. C.; Griesser, H. J. *Surf. Interface Anal.* **1996**, *24*, 271−281.

(45) Kemnitz, C. R.; Loewen, M. J. *J. Am. Chem. Soc.* **2007**, *129*, 2521−2528.

(46) Hollahan, J. R.; Bell, A. T. *Techniques and applications of plasma chemistry*; Wiley: New York, 1974; Vol. *VIII*.

(47) Lee, J. H.; Jung, H. W.; Kang, I. K.; Lee, H. B. *Biomaterials* **1994**, *15*, 705−711.